FY2012 EHP Program Announcement 12HQPAQ0001

Final Technical Report

Award # G12AP20031

The Intraplate Earthquake Cycle:
Strain and Displacement Behavior during the
Canterbury, NZ Earthquake Sequence

Kevin P Furlong
Department of Geosciences
Pennsylvania State University
543 Deike Building
University Park, PA 16802

(814) 863-0567 (Tel)
(814) 863-7823 (Fax)
kevin@geodyn.psu.edu

Project Duration:
January 1, 2012 - December 31, 2012

Abstract

How does crustal deformation progress through the earthquake cycle in intraplate regions?

This was the fundamental question we addressed in this research. The recent and ongoing Canterbury NZ earthquake sequence has provided an ideal opportunity to investigate this question and advance our understanding of both how earthquakes 'work' in intraplate regions and what observables will help us identify other at-risk locations. Implicit in this question is the corollary that there are differences between crustal deformation behavior in *interplate* and *intraplate* regimes. Our results show that in contrast to *interplate* systems that are well described by a *displacement driven* earthquake cycle, the Canterbury NZ *intraplate* system reflects a *stress driven* earthquake cycle. Among the principal results we have obtained during this 12-month project are:

1. Observed surface fault slip is in systematic agreement with fault slip inferences obtained seismologically with finite-fault models (FFM), although in regions of maximum observed surface slip, displacement magnitudes exceed those determined through the FFMs. In regions where the seismologic FFMs indicate little or no shallow slip (upper 1-2 km), there is no localized surface fault rupture, although other geophysical evidence supports the subsurface fault slip determined by the FFMs.
2. We determined 146 Regional Moment Tensors for the main earthquake event and the larger aftershocks (minimum Mw = 3.8). 121 of these events fall within the strike-slip fault category. With the exception of earthquakes at the extreme western and eastern ends of the aftershock region, essentially all RMT focal mechanisms show E-W right-lateral (or equivalently N-S left-lateral) fault motion. In most cases, the E-W fault strike is assumed to be the actual rupture plane for compatibility with the E-W strike of the observed surface faulting and the aftershock patterns.
3. There is no change in orientation of the local-regional stress field in either time or space during the 2+ year earthquake sequence.
4. Modeling fault slip as determined by seismologic FFMs for comparison with observed InSAR crustal deformation indicates that there is a substantial right-step in the mainshock rupture (near the eastern end of the observed surface rupture). This co-seismic step-over in the rupture exceeds 8-10 km in distance and is significantly larger than typically assumed. A complex and long-lived pattern of aftershock activity (dominated by strike-slip (not Normal) faulting) has occurred in that right-step, step-over zone.
5. Aftershock activity on fault segments not involved in the initial main rupture are focused in space and time, and not re-activated by subsequent nearby large aftershocks.

Regional Setting and Science Questions

The recent Mw 7.0 Canterbury (Darfield) NZ earthquake[1] in September, 2010 and its ongoing aftershock sequence, including the extremely damaging Mw 6.1 Christchurch earthquake during February of 2011 provide a setting to evaluate the appropriateness of standard earthquake cycle deformation models for such intra-plate earthquakes (Figure 1). This earthquake and its aftershocks have been a fundamental game-changer for earthquake hazards studies in New Zealand; prior to this event, the Christchurch area was thought to be susceptible to earthquake hazards primarily from the strong shaking effects of large, but relatively far-field (i.e. > 100km away) events on the Alpine Fault and Marlborough Fault system. The effects of this earthquake sequence clearly demonstrate the extreme consequences of even relatively small events (Mw 6.1) on a modern, relatively well-prepared city; and as a result point out the need to better understand the underlying causes of such events and whether there may be diagnostic observations that would allow similar at-risk regions to be identified.

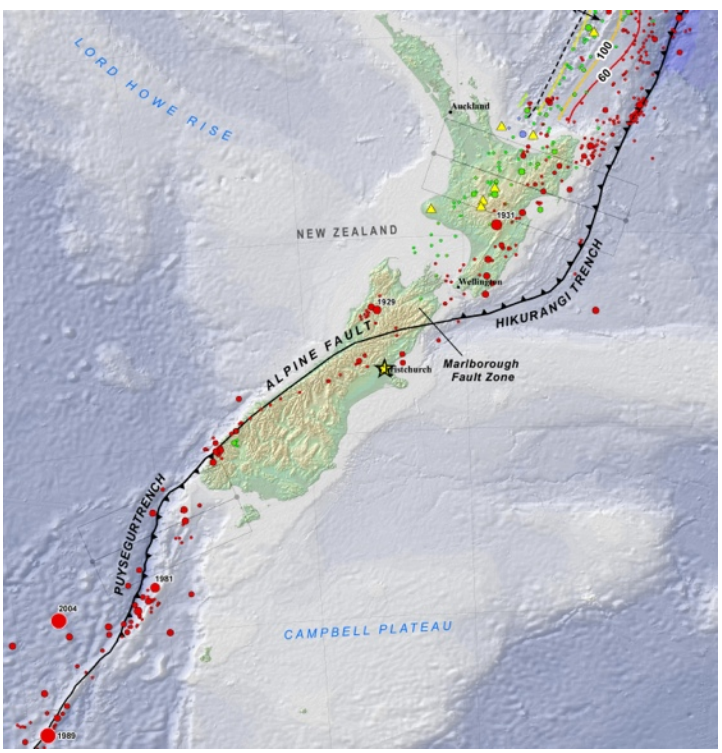

Figure 1. Tectonic setting of the Canterbury earthquake sequence in New Zealand. Previous earthquake hazard analyses in NZ had focused on either plate boundary structures such as the Alpine Fault and Hikurangi Subduction zone, or subsidiary faults associated with main plate boundary structures (e.g. Wellington Fault, in upper plate of the subduction zone). The Canterbury sequence, (although stresses driving the deformation are ultimately related to plate interactions), is essentially an intraplate earthquake sequence - failure of a sequence of relatively small offset faults - and thus it provides an ideal opportunity to quantify aspects of strain accumulation and release in intraplate regions such as Central US.

As is described in more detail later in this report, the Greendale Fault,

[1] There is a systematic discrepancy between magnitudes determined by USGS-NEIC and GeoNet (NZ). GeoNet magnitudes are systematically greater - typically 0.2 to 0.4 magnitude units larger. We use USGS magnitudes, when available. In our analyses, we developed a consistent set of magnitudes for all 146 events analyzed. Our magnitudes are in general agreement with NEIC magnitudes and systematically lower than NZ GeoNet magnitudes.

along which the main Mw 7.0 earthquake occurred, is a series of fault segments (of uncertain connectivity) that ruptured during the event (Figure 2). Although these fault segments were almost certainly pre-existing and had likely experienced previous events, in general they are relatively small-offset faults. They have not developed into a through-going fault system, such as we see as faults mature and link along the San Andreas System. In spite of the segmented nature of the faults in the Canterbury case, this earthquake sequence demonstrates that even small-offset, discontinuous fault segments can combine in a variety of ways and host damaging earthquakes that can devastate a modern city.

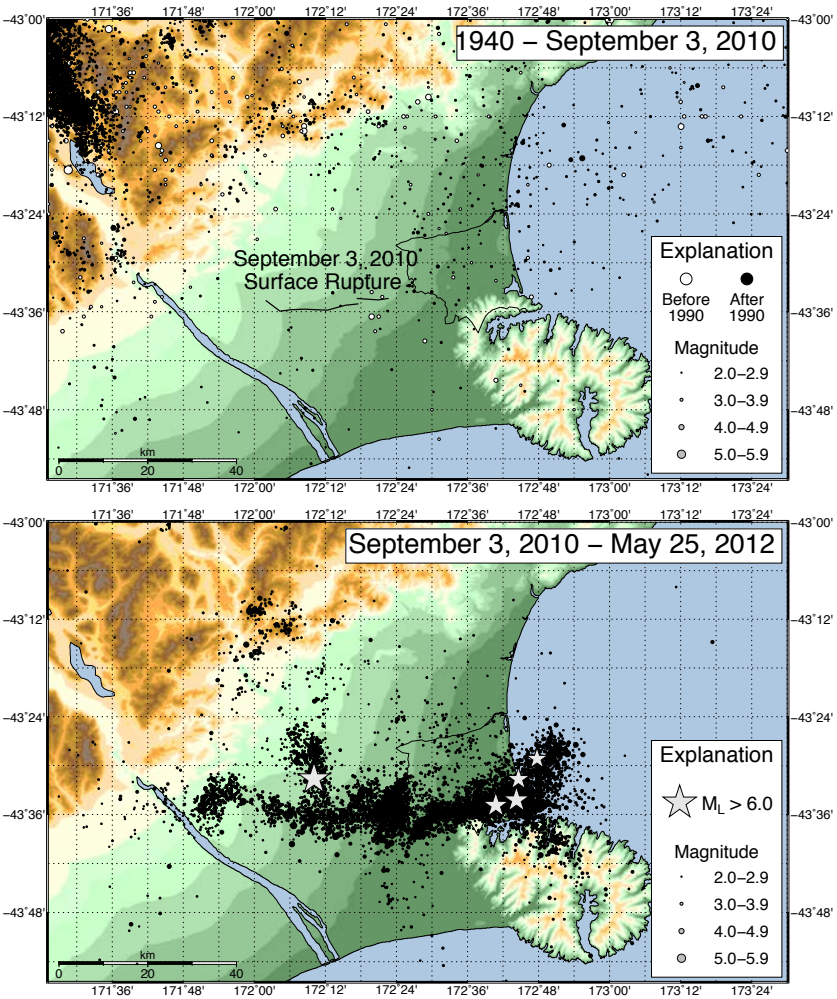

Figure 2. Seismicity behavior of the Canterbury region. (Top) Panel shows the background seismicity for the region for an ~ 70 year time period prior to main rupture in September 2010 (the future Greendale Fault surface rupture is shown in as black line segments). (Bottom) Panel shows the seismicity associated with the main Mw 7.0, September 3 event; until end of March, 2012. The epicenters (NZ GeoNet location) of the main event and the largest aftershocks are shown by stars.

Regional Moment Tensors - Methods and Results

We created a simple one-dimensional velocity model for waveform inversion appropriate for regional wave propagation through South Island, thereby improving the robustness of the moment tensor solutions and allowing the analysis of smaller events. The presence of dispersed surface waves at distant stations (>250 kilometers) on South Island suggested we use the inversion tools developed by Herrmann and Ammon (2004) to compute a regional one-dimensional velocity structure. We calculated

group velocities using multiple filter analysis on vertical and transverse waveforms, yielding Rayleigh and Love wave dispersion measurements in the 5-50 second period range (Herrmann 1973; Herrmann et al., 2011b). The velocity model inversion was initialized with a Canterbury Basin velocity-depth profile (Van Avendonk et al., 2004). The inversion produced a one-dimensional South Island, New Zealand velocity model (SINZ) averaging over all the South Island geological structure sampled by surface waves.

The time domain regional moment tensor inversion of Herrmann et al., (2011a), relies on fitting synthetic waveforms to seismograms observed at regional broadband stations on South Island. The New Zealand Seismograph Network provides azimuthal coverage greater than 180° for all but the smallest offshore events in the Canterbury sequence, allowing us to capture the earthquake radiation patterns. Three-component raw digital waveforms were deconvolved to ground velocity, in m/s, and rotated to vertical, radial, and transverse components (Herrmann et al., 2011a). These traces were truncated at 10 seconds prior to the P wave arrival and 120 seconds after the P wave arrival, and then filtered from 0.02-0.0625 Hz (Herrmann et al., 2011a). Waveforms from events larger than ~M_W5.5 were filtered to shorter periods (0.01-0.033 Hz) to maintain the validity of the point source approximation. The dominant contributions to these bandpass-filtered waveforms from the shallow crustal earthquakes in the Canterbury sequence were typically the fundamental mode Rayleigh (on the vertical and radial components) and Love (on the transverse component) surface waves (Herrmann et al., 2011a).

A best-fitting double couple source was found by performing a systematic grid search over strike, dip, and rake, in increments of 5°, and source depth, in increments of 1 kilometer (Herrmann et al., 2011a). Full moment tensor inversions for several of these earthquake indicate that the double couple approximation is valid. At each depth, predicted ground velocity waveforms at the station locations were generated for each set of strike, dip, rake, and source depth from precomputed Green's functions corresponding to the SINZ model (Herrmann et al., 2011a; Herrmann et al., 2011b). A regional moment tensor moment magnitude (M_W^{RMT}) was computed for the best double couple source parameters at each depth by minimizing the least-squares misfit between the predicted waveforms, scaled by the seismic moment, and the observed waveforms (Herrmann et al., 2011a).

Our moment magnitude estimates are consistently M 0.1-0.2 smaller than GeoNet, Global CMT, and USGS WPhase moment magnitudes. The most likely difference is our choice of velocity structure, which could lead to systematic magnitude differences of this size. However, our focal mechanisms typically match teleseismic solutions and GeoNet regional solutions closely. The major exception is the September 3, 2010 main

shock: our focal mechanism is right lateral strike slip, whereas the GeoNet solution has a thrust solution. The waveform fits at stations on South Island are significantly better for a right lateral strike slip source than for the GeoNet thrust source.

The focal mechanisms (Figure 3) for events in the Canterbury sequence range from strike slip to reverse, and include only two normal faulting events. Strike slip earthquakes dominate the sequence: 121 focal mechanisms are classified as dominantly strike slip (Frohlich, 1992). By inspection, most of these strike slip focal mechanisms have nodal planes accommodating either right lateral slip on planes striking E-ENE, or left lateral slip on planes striking S-SSE, but several of these strike slip earthquakes contain nodal planes rotated up to 45° from this dominant orientation. Most of the reverse focal mechanisms have nodal planes accommodating slip on planes striking SW-NE.

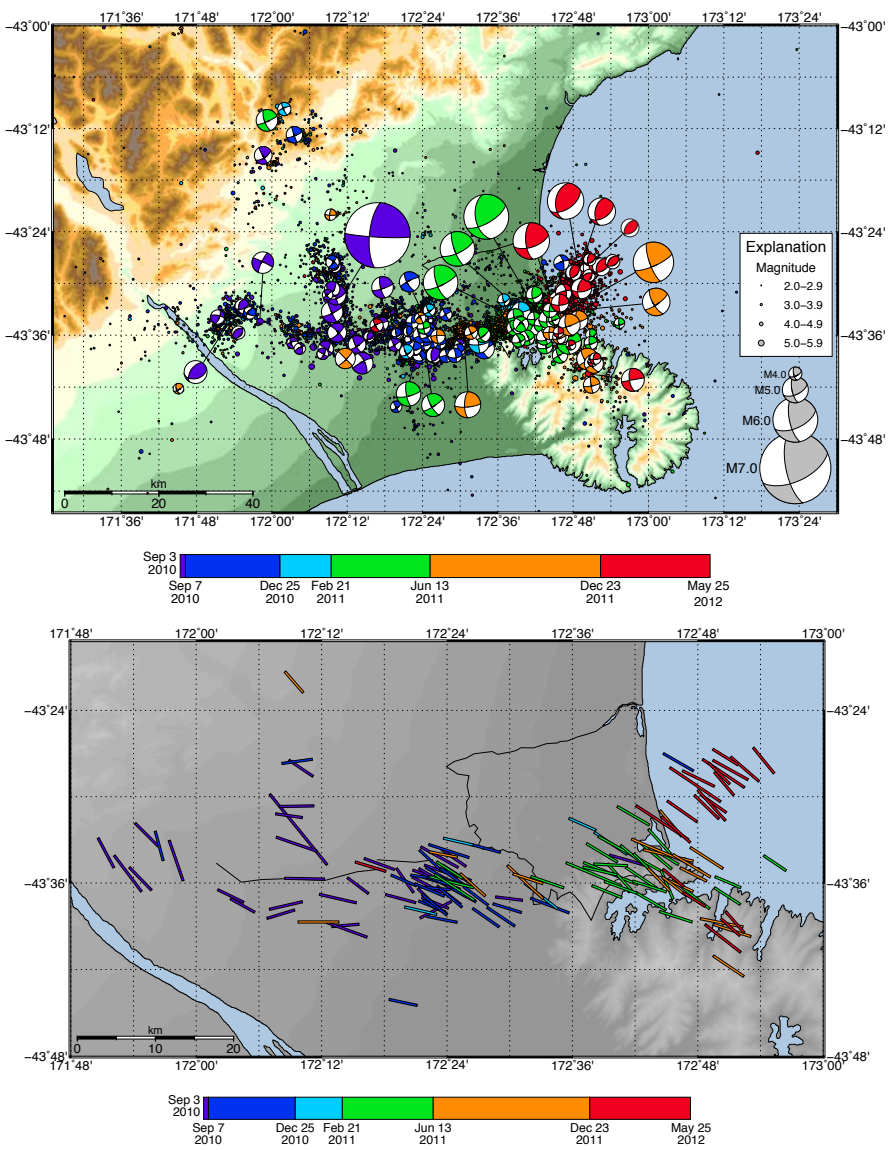

Figure 3. (Upper) Focal mechanisms from our RMT solutions for the larger aftershocks in the 2010-2012 Canterbury sequence. Mechanisms are color coded according to time of the event. (Lower) P-axis from focal mechanisms. Note the consistency in space and time of the p-axis orientations.

Although the Canterbury earthquake sequence was comprised of multiple short and diffuse fault segments with varying orientations and kinematics, the focal mechanisms are dominantly compatible with a single, uniform stress field that remains unchanged throughout the duration of the

sequence. The P-axes of these focal mechanisms (Figure 3) have nearly uniform orientations over time and space, indicating a nearly horizontal σ_1, oriented at N115ºE. Strike slip earthquakes account for most of the moment release throughout the sequence (~80%), suggesting σ_3 is also horizontal, oriented at N25ºE, i.e. the system is an Andersonian wrench faulting regime (Anderson, 1905). This stress field is consistent with geologic and geophysical stress indicators in eastern (intraplate) South Island determined prior to the Canterbury earthquake sequence (Sibson et al., 2011). Although there is a large imbalance in favor of strike-slip earthquakes, the presence of oblique to reverse focal mechanisms may indicate $\sigma_2 \approx \sigma_3$ in the Canterbury Plains (Sibson et al., 2011). The diversity of fault orientations and earthquake kinematics suggests that this stress field is reactivating hidden preexisting structures in the subsurface with compatible orientations. In this interpretation, the predominance of right lateral strike slip earthquakes suggests that the subsurface is dominated by nearly vertical faults striking ENE.

There is no evidence in these seismic focal mechanisms for significant regional perturbations to the stress field following the M_W7.0 or M_W6.0 ruptures in the Canterbury sequence. In similar earthquake sequences occurring near plate boundaries, e.g. the 1992 M_W6.1 Joshua Tree and M_W7.3 Landers sequences, σ_1 indicated by earthquake focal mechanisms rotated 10º-20º following the main ruptures. This reflects the strain and stress release that accompanies an earthquake rupture and is predicted by the elastic rebound model. Although we did not perform a full stress tensor inversion from the focal mechanisms in the Canterbury sequence, the constant orientation of σ_1 suggests that it is not changing following the major ruptures. This may reflect the intraplate deformation and seismogenic process, where a rupture inside a slowly-deforming region does not significantly perturb the stress that has accumulated. The hazard implications of this are significant: although the seismic hazard in low-strain intraplate settings is lower than in rapidly-deforming plate boundary settings, the hazard may not decrease in the same way after a large earthquake. Instead, the earthquake cycle in intraplate South Island may consist of multiple Canterbury-like sequences, with long recurrence intervals on any one set of faults.

Aftershock Seismicity

Since the initial rupture, over 10,000 aftershocks with M_L2.0 and greater have been recorded in the GNS Science database, including 40 events greater than M_L5.0 (Figures 3, 4). Although all of the events can be correctly labeled aftershocks of the September M_W 7.0 event, there were four decaying aftershock sequences corresponding to the four largest events (~MW6.0) on February 21, June 13, and a pair of earthquakes on December 23, 2011 (Figure 4). The vast majority of aftershocks occurred within 2-3

weeks of each of these four events (Figure 4). The aftershocks did not cluster onto planar faults, even with careful locations within a local strong motion network or relocation techniques applied to the hypocenters, suggesting the events occurred on many structures in the subsurface, rather than on one master fault (Bannister et al., 2011).

The September 3, 2010 M_W^{RMT}6.8 (USGS M_W7.0) main shock of the Canterbury earthquake sequence had a pure strike slip focal mechanism, with a ~30 kilometer long surface rupture clearly delineating the right lateral east-striking fault plane and indicating a ~N90ºE slip vector (Figure 3). However, none of the aftershocks in our catalog exactly matched this main shock focal mechanism, and it was evident from multiple surface rupture segments, bands of aftershocks, and aftershock focal mechanisms that the deformation near the surface rupture was more complex than simply right lateral slip on a single, ~N90ºE striking plane (Figure 3). two small aftershocks (M_W^{RMT}3.9 and 4.2) with reverse mechanisms near the main shock epicenter were compatible with NZ seismological (Gledhill et al., 2011) and geodetic (e.g. Beavan et al., 2010) interpretations that the main rupture initiated as a reverse faulting event north of the surface rupture.

There were three primary segments of aftershocks in the eastern side of the Canterbury earthquake sequence, corresponding to the February 21, June 13, and December 23, 2011 Christchurch earthquakes, as well as sparser aftershock activity between the eastern end of the surface rupture and the city of Christchurch. Following the September 2010 main shock, a narrow band of aftershocks extended ENE between the major dextral stepover and Christchurch (Figure 3, 4). Focal mechanisms of aftershocks in this segment indicated right lateral strike slip deformation, with slip vectors oriented ~N75ºE (Figure 3, 5). The February 21, 2011 M_W^{RMT}6.0 (USGS M_W6.1) Christchurch event was oblique, although most of its aftershock focal mechanisms were pure strike slip, with similar orientations to the focal mechanisms from the events prior to February 2011 (Figure 3). The June 13, 2011, M_W^{RMT}5.8 (USGS M_W6.0) earthquake occurred ~5 kilometers east of the February 21, 2011 epicenter, with a pure strike slip focal mechanism resembling the foreshocks and aftershocks of the February event (Figure 3). Interpreting the fault plane for the June 2011 event was problematic, because there were two dense aftershock arrays parallel to each of the nodal planes (Figure 3, 4). We interpreted the June 2011 earthquake and aftershocks as dominantly left lateral, on a conjugate structure striking ~N150ºE and extending onto Banks Peninsula for two reasons: (a) the highest density of aftershocks occurred along this SSE arm, and (b) the largest aftershocks of the event were located in the middle of Banks Peninsula, lying within this SSE arm of aftershocks (Figure 4). However, it is possible that the June 2011 main shock jointly ruptured both the ENE and SSE planes. These left lateral earthquakes had nearly uniform slip vectors

oriented at N150º-165ºE, or 60º-90º from the February 2011 sequence slip vectors (Figure 3).

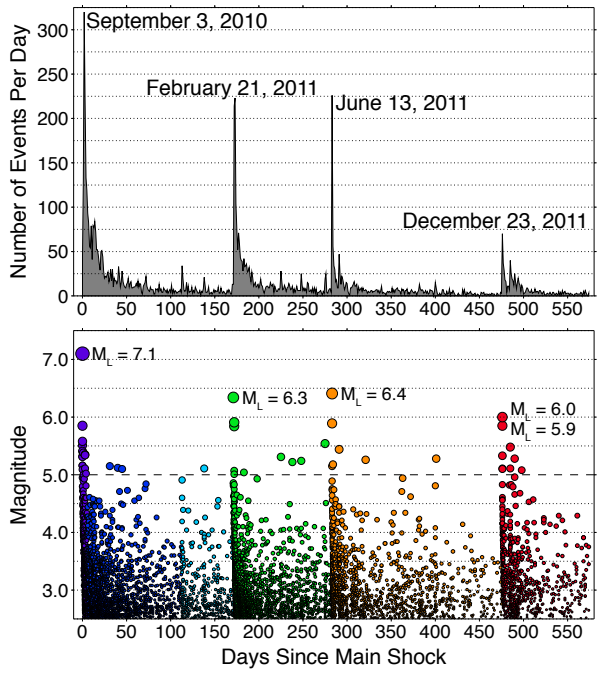

Figure 4. (Upper) Time sequence of aftershocks in the Canterbury Sequence. General Omori-like decay for each large-shock - aftershock sequence, but no overall simple decay pattern after main shock. (Lower) Map views of seismicity, color-coded by time. Each time slice reflects the time of a large-shock - aftershock period. In general there is little re-activation of previously ruptured fault patches by subsequent nearby major aftershocks.

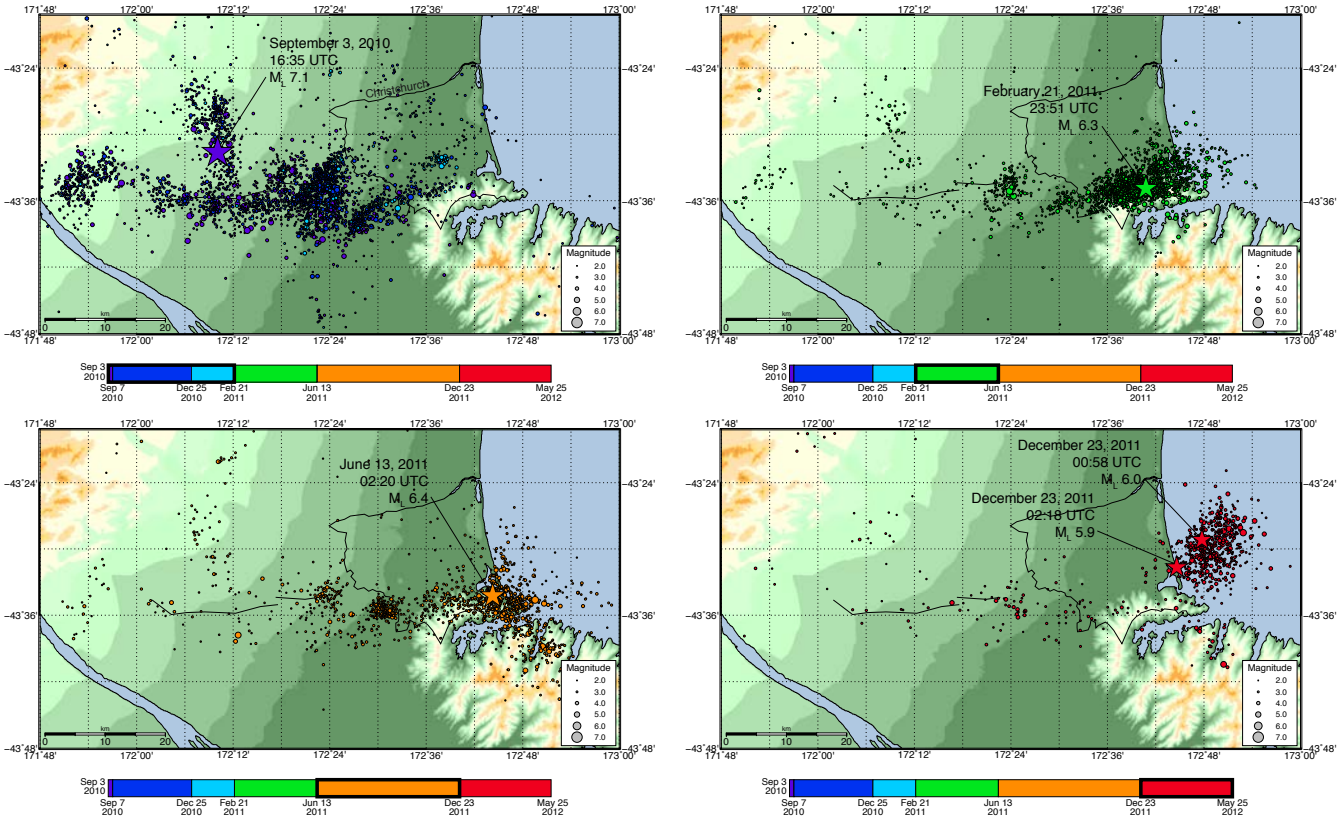

On December 23, 2011, two M_W^{RMT}5.6 (USGS M_W5.8 and M_W5.9) earthquakes ruptured offshore east of Christchurch: the first occurred ~10 kilometers northeast of the June 2011 epicenter, and had a reverse focal mechanism (Figure 3,4); the second occurred two hours later only ~5 kilometers northeast of the June 2011 epicenter, and had a strike slip focal mechanism resembling the June 2011 main shock focal mechanism (Figure 3). Unlike the narrow aftershock bands corresponding to the February and June 2011 earthquakes (Figure4), the aftershock array corresponding to the December 2011 events was broad, due to the non-vertical dip of the structure, and extended generally northeast (Figure 3, 4). The slip directions for the events with reverse focal mechanisms were consistently rotated ~20° clockwise from the slip vectors for events with strike slip focal mechanisms (N90°-105°E; Figure 3).

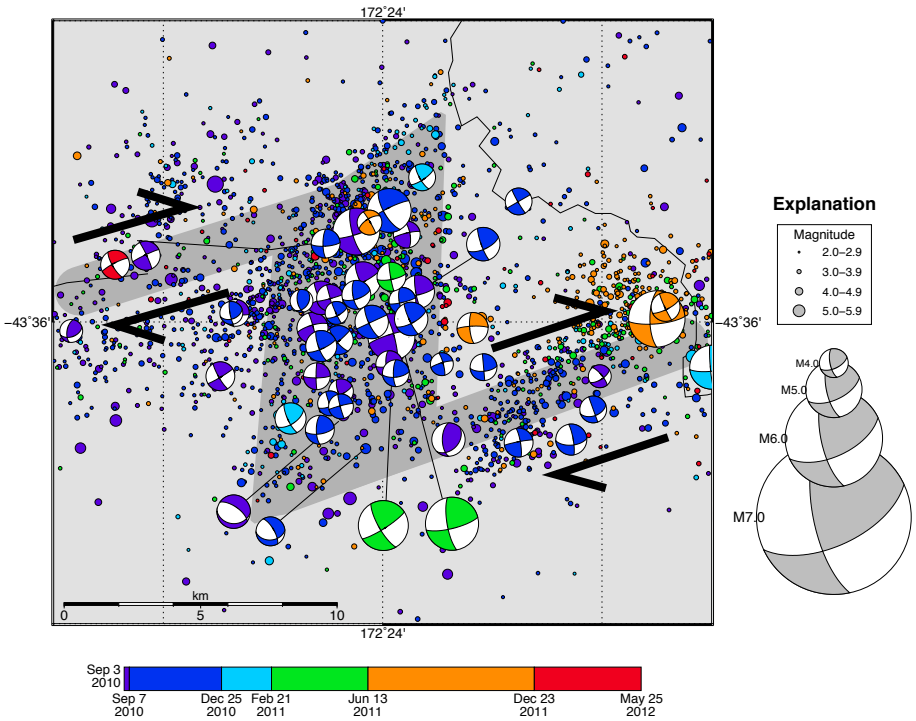

Figure 5. Ongoing seismicity in the major step-over region near the eastern end of the surface rupture of the Greendale Fault. This right-step would normally be assumed to involve a pull-apart or extensional deformation but is characterized by dominantly strike-slip faulting. Note also that this is the one region of the initial rupture that has maintained activity throughout the Canterbury sequence.

Separating the western side of the Canterbury earthquake sequence from the eastern side was a ~10 kilometer releasing step, clearly apparent on the map as a polygon of intense aftershock activity (Figure 5). Our regional moment tensor catalog contained only two events with normal faulting focal mechanisms in the step-over region, and there was no evidence for subsidence. All of the 41 other regional moment tensors we calculated within the step-over had almost the exact same strike slip focal mechanisms, with magnitudes ranging from M_W^{RMT}3.7-4.9 (Figure 5). There were no linear aftershock trends within the zone, so that interpreting the fault planes for these focal mechanisms was nearly impossible. Sibson (1986), discussed several similar instances in California and Iran where strike slip aftershock activity following M 6.0-7.0 strike slip earthquakes was concentrated

within major releasing steps, without significant normal faulting. These zones of strike slip activity were typically a few kilometers in length and width (Sibson, 1986), putting them on a similar scale as the major releasing step of the Canterbury earthquake sequence. Sibson, (1986) proposed that the internal structure of such a releasing step would be a network of short, conjugate strike slip segments, including both right lateral and left lateral fault segments, connected by minor extension fractures. Such a structure would account for (a) the scarcity of normal faulting events and (b) the relatively small maximum magnitude (less than M_W^{RMT}5.0) of the strike slip events within the zone.

Fault Geometry and Kinematics

The Greendale Fault is one of the most completely observed strike-slip surface ruptures (Quigley et al., 2012). The subsurface rupture has also been well imaged with a Finite Fault Model (USGS NEIC; Hayes, 2010) (Figure 6). This provides an opportunity to correlate the observed surface rupture with the imaged subsurface rupture for geometry, extent, and magnitude.
Only the western 30 km of the September 3, 2010 rupture extended to the surface and the observed surface slip exceeds that inferred from seismologic models for the shallow subsurface fault by a factor of ~ 2. Whether this reflects the choice of material properties in the seismologic model - Seismic Moment is modeled and converted to fault slip based on fault geometry and assumed fault zone properties - or is an accurate representation of the co-seismic fault slip remains unresolved.

It is also important to note that the eastern 20 km of co-seismic rupture is not included in the surface faulting inventory. As seen in Figures 4 and 5, there was substantial aftershock activity in the region east of the surface rupture, and some of the strongest measured co-seismic strong motions were observed in that region. There is continuing debate as to whether the fault extends beyond the observed surface rupture. It is quite typical for large segments of strike-slip faults to not rupture to the surface, so it would be a special case if the Greendale Fault exhibited complete surface rupture. Similarly the aftershock behavior and the complex and continuing activity in the right-step, step-over region just to the east of the end of the surface rupture (Figures 3,4,5). We believe the strongest evidence for the continuation of co-seismic rupture to the east beyond the observed surface rupture is seen in the InSAR observations of the rupture area.

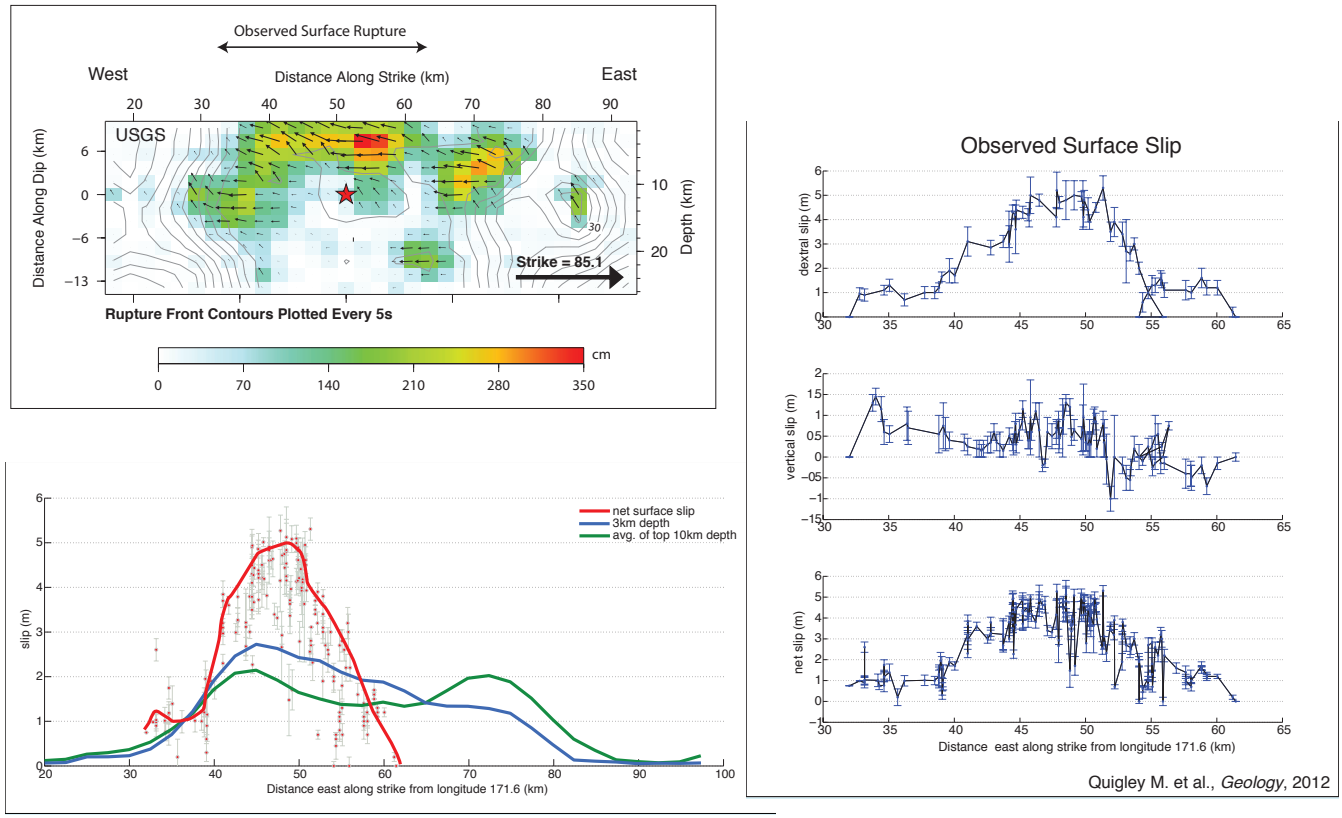

Figure 6. Correlation of observed surface displacements on Greendale Fault (Upper right from: Quigley et al, 2012) and subsurface slip from USGS FFM (Upper left from USGS Hayes, 2010). Note only~ 2/3 of fault rupture included surface rupture (Lower left). Eastern segment (from position 60 km to the east in FFM) was not observed at surface.

In Figure 7, observed and modeled InSAR results for the region are shown. The Elliott et al. (2012) results shown are similar to all others available. They show a distinct difference between the interferogram observed by an ~ eastward view (upper left in Figure 7) as compared to the ~ westward view (lower left, Fig. 7). The main observed rupture along the Greendale Fault was nearly E-W, right lateral faulting with the south side slightly up (Figure 6); the easternmost segment of the surface rupture was still E-W right lateral, but with the north side up. This pattern of displacement would result in the InSAR patterns observed - the East looking image would see a coherent pattern of line-of-site (LOS) ground motion over the fault segments with south side up, but the displacements would be muted where north-side is up. In a similar fashion the west looking LOS image will primarily image the fault segments with north side up (i.e. the eastern surface rupture and any other regions of similar kinematics). The lack of good coherency in the west looking views has led other groups to focus primarily on the east looking LOS imagery. We find that including the eastern extent of subsurface rupture as seen in the USGS FFM for the event (Figure 6, position 60 km to the east) in our InSAR analyses reproduces reasonably well the observed pattern for both the east and west looking views. (Figure 7, right hand panels). In these models, displacements implied by the seismologic FFM are converted to equivalent InSAR interferograms. Best

correlations come when the eastern fault segment is offset to the south by 5-10 km as shown in Figure 5.

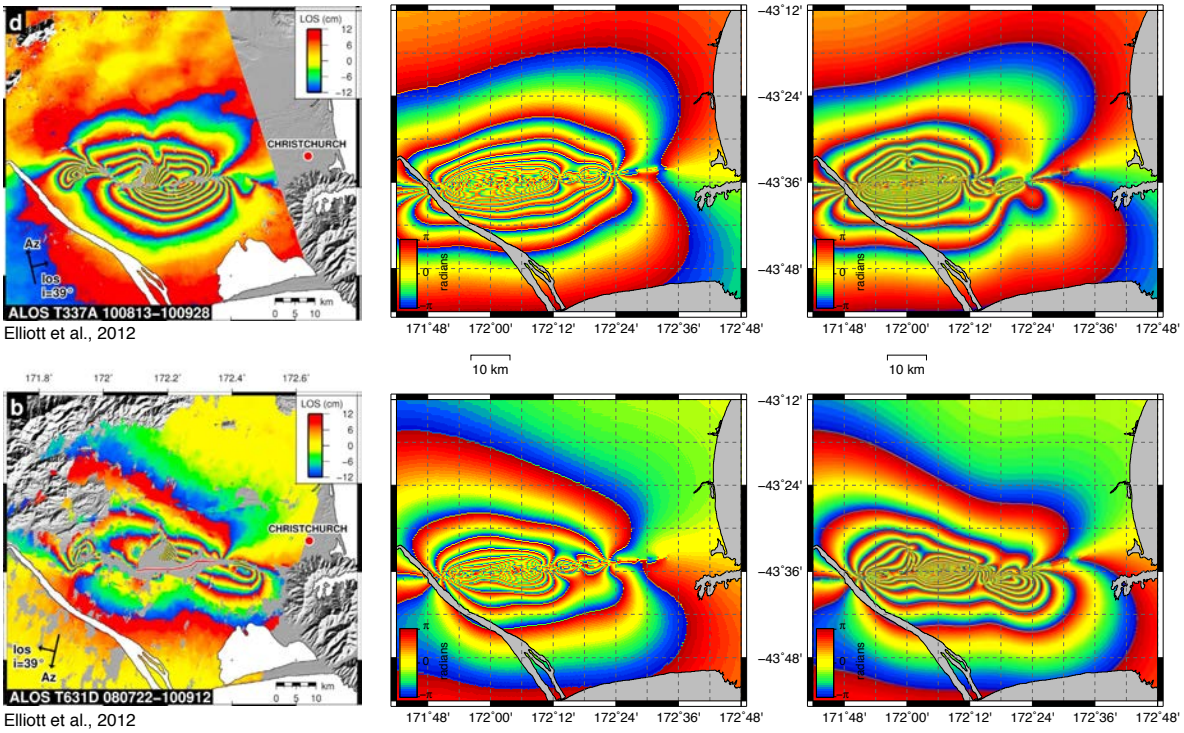

Figure 7 Comparison of observed surface displacements seen in InSAR interferograms for the September 2012 events (Elliott et al, 2012) with models derived from the USGS Finite Fault model displacements. Upper panels are for east looking LOS views and lower panels are west looking LOS views. Center panel shows model results for FFM with no offset on eastern segment and all sections having south-side up. Right hand panels show InSAR results with a offset of the eastern fault segment to the south; with the eastern segments having a north-side up component. The southern offset and shift in vertical motion, consistent with seismicity, strong motion amplitudes and observed displacements on the easternmost segment of surface rupture. provide a reasonable correlation to observed interferograms. [Note - Models derived from the FFM are geo-located based on the assumed initiation point of rupture and rupture velocity. As a result there may be systematic shifts in patterns but spatial patterns should remain robust.]

Overview and Conclusions

How does crustal deformation progress through the earthquake cycle in intraplate regions?

This was the fundamental question we addressed in this research. The recent and ongoing Canterbury NZ earthquake sequence has provided an ideal opportunity to investigate this question and advance our understanding of both how earthquakes

'work' in intraplate regions and what observables will help us identify other at-risk locations. Among the principal results we have obtained during this 12-month project are:

1. Observed surface fault slip is in systematic agreement with fault slip inferences obtained seismologically with finite-fault models (FFM), although in regions of maximum observed surface slip, displacement magnitudes exceed those determined through the FFMs. In regions where the seismologic FFMs indicate little or no shallow slip (upper 1-2 km), there is no localized surface fault rupture, although other geophysical evidence supports the subsurface fault slip determined by the FFMs.
2. We determined 146 Regional Moment Tensors for the main earthquake event and the larger aftershocks (minimum Mw = 3.8). 121 of these events fall within the strike-slip fault category. With the exception of earthquakes at the extreme western and eastern ends of the aftershock region, essentially all RMT focal mechanisms show E-W right-lateral (or equivalently N-S left-lateral) fault motion. In most cases, the E-W fault strike is assumed to be the actual rupture plane for compatibility with the E-W strike of the observed surface faulting and the aftershock patterns.
3. There is no change in orientation of the local-regional stress field in either time or space during the 2+ year earthquake sequence.
4. Modeling fault slip as determined by seismologic FFMs for comparison with observed InSAR crustal deformation indicates that there is a substantial right-step in the mainshock rupture (near the eastern end of the observed surface rupture). This co-seismic step-over in the rupture exceeds 8-10 km in distance and is significantly larger than typically assumed. A complex and long-lived pattern of aftershock activity (dominated by strike-slip (not Normal) faulting) has occurred in that right-step, step-over zone.
5. Aftershock activity on fault segments not involved in the initial main rupture are focused in space and time, and not re-activated by subsequent nearby large aftershocks.

References Cited in Report

Anderson, E.M., 1905. The dynamics of faulting. *Transactions of the Edinborough Geological Society* 8, 387-402.

Bannister, S., B. Fry, M. Reyners, J. Ristau, and H. Zhang, 2011′ Fine-scale relocation of aftershocks of the 22 February M6.2 Christchurch earthquake using double-difference tomography, *Seismological Research Letters V. 82,* Num. 6, 839-845; doi: 10.1785/gssrl.82.6.839

Beavan, J., Samsonov, S., Motagh, M., Wallace, L., Ellis, S., and Palmer, N., 2010. The Darfield (Canterbury) earthquake: Geodetic observations and preliminary source model. *Bulletin of the New Zealand Society for Earthquake Engineering* 43, 228-235.

Frohlich, C., 1992. Triangle diagrams: ternary graphs to display similarity and diversity of earthquake focal mechanisms. *Physics of the Earth and Planetary Interiors* 75, 193-198.

Gledhill, K., Ristau, J., Reyners, M., Fry, B., and Holden, C., 2011. The Darfield (Canterbury, New Zealand) M_W 7.1 earthquake of September 2010: A preliminary seismological report. *Seismological Research Letters* 82, 378-386.

Hayes, G.P., 2010, Finite Fault Model: Updated Result of the Sep 3, 2010 Mw 7.0 Darfield, South Island New Zealand Earthquake; http://earthquake.usgs.gov/earthquakes/eqinthenews/2010/us2010atbj/finite_fault.php

Herrmann, R.B., 1973. Some aspects of band-pass filtering of surface waves. *Bulletin of the Seismological Society of America* 63, 703-711.

Herrmann, R.B., and Ammon, C.J., 2004. Computer programs in seismology–3.30: GSAC–Generic seismic application coding. http://www.eas.slu.edu/eqc/eqccps.html.

Herrmann, R.B., Benz, H., and Ammon, C.J., 2011a. Monitoring the earthquake source process in North America. *Bulletin of the Seismological Society of America* 101, 2609-2625.

Herrmann, R.B., Malagnini, L., and Munafo, I., 2011b. Regional moment tensors of the 2009 L'Aquila earthquake sequence. *Bulletin of the Seismological Society of America* 101, 975-993.

Quigley, M., Van Dissen, R., Litchfield, N., Villamor, P., Duffy, B., Barrell, D., Furlong, K., Stahl, T., Bilderback, E., and Noble, D., 2012. Surface rupture during the 2010 M_W 7.1 Darfield (Canterbury) earthquake: Implications for fault rupture dynamics and seismic-hazard analysis. *Geology* 40, 55-58.

Sibson, R.H., 1986. Rupture interaction with fault jogs. In *Earthquake Source Mechanics*, ed. S. Das, J. Boatwright, and C.H. Scholz, 157-167. American Geophysical Union Monograph 37 (Maurice Ewing Series 6). Washington, D.C: American Geophysical Union.

Sibson, R., Ghisetti, F., and Ristau, J., 2011. Stress control of an evolving strike-slip fault system during the 2010-2011 Canterbury, New Zealand, earthquake sequence. *Seismological Research Letters* 82, 824-832.

Van Avendonk, H.J.A., Holbrook, W.S., Okaya, D., Austin, J.K., Davey, F., and Stern, T., 2004. Continental crust under compression: A seismic refraction study of South Island Geophysical Transect I, South Island, New Zealand. *Journal of Geophysical Research* 109, B06302.

Bibliography of Publications Under Project

Papers Related to NEHRP project:

Quigley, M., R. Van Dissen, N. Litchfield, P. Villamor, B. Duffy, D. Barrell, **K. Furlong**, T. Stahl, E. Bilderback, and D. Noble,, 2012, Surface rupture during the 2010 M w 7.1 Darfield (Canterbury) earthquake: Implications for fault rupture dynamics and seismic-hazard analysis, *Geology,* v. 40; no. 1; p. 55–58; doi:10.1130/G32528.1

Villamor, P., N Litchfield, D Barrell, R Van Dissen, S Hornblow, M Quigley, S Levick, W Ries, B Duffy, J Begg, D Townsend, T Stahl, E Bilderback, D Noble, **K Furlong** and H Grant, 2012, Map of the 2010 Greendale Fault surface rupture, Canterbury, New Zealand: application to land use planning, *New Zealand Journal of Geology and Geophysics*, DOI:10.1080/00288306.2012.680473

Abstracts of presentations of NEHRP project research

Herman, Matthew W.; Kevin P. Furlong; Robert B. Herrmann; Harley Benz
Using Regional Moment Tensors to Constrain the Kinematics and Stress Evolution During the 2010-2012 Canterbury, New Zealand, Earthquake Sequence
Abstracts of papers at 2012 AGU Fall Meeting T33A-2644.

Meyers, Beth; Kevin P. Furlong; Gavin P. Hayes; Matthew W. Herman; Mark Quigley
Surface and Subsurface Fault Displacements from the September 2010 Darfield (Canterbury) Earthquake
Abstracts of papers at 2012 AGU Fall Meeting T33A-2645.